A Comparison of POCS Algorithms for Tomographic Reconstruction Under Noise and Limited View

FERNANDO V. SALINA[1], NELSON. D. A. MASCARENHAS[1], PAULO E. CRUVINEL[2]

[1]UFSCar – Universidade Federal de São Carlos, Caixa Postal 676, 13565-905 São Carlos, SP, Brasil
{salina,nelson}@dc.ufscar.br
[2]EMBRAPA-CNPDIA – Empresa Brasileira de Instrumentação Agropecuária – Centro Nacional de Pesquisa e Desenvolvimento de Instrumentação Agropecuária, R. XV de Novembro, 1452, 13560-970 São Carlos, SP, Brasil
cruvinel@cnpdia.embrapa.br

Abstract. We present in this work a comparison among four algorithms for transmission tomography. The algorithms are based on the formalism of POCS (Projection onto Convex Sets): ART (Algebraic Reconstruction Technique), SIRT (Simultaneous Iterative Reconstruction Technique), sequential POCS and parallel POCS. We found that the use of adequate a priori knowledge about the solutions, expressed by convex sets restrictions, particularly in the case of the last algorithm, is an efficient way to reduce the variations on the solutions due to the ill-conditioning of the reconstruction problem, not only due to the noise in the projections, but also due to limited view reconstruction.

1. Introduction

Several problems in image processing, as tomographic reconstruction or image restoration, can be efficiently solved if restrictions are imposed over the set of possible solutions. Under certain conditions, the restrictions can also be considered as sets.

One way to impose these restrictions is to use the method of projections. If the sets that represent the restrictions are convex, it is possible to find the solution of the problem, which is represented by the intersection of the sets (if it exists).

2. Transmission Tomography

Transmission tomography consists basically in irradiating the object in several directions and storing for each direction the transmitted and received intensities. To accomplish that, a collimated beam of radiation is used, which defines vertical planes as thin as the beam itself. The emitted and received intensities are stored and in this way we obtain a longitudinal view of the object. By using several collimated parallel beans, we obtain several vertical planes, which define profiles in several angular positions. These stored values can be processed to create a matrix,, called image, where each entry represents the linear attenuation coefficient at a certain position.

From the mathematical point of view, the solution for the problem of reconstruction of a function from line integrals was solved by Radon in 1917 [1]. However, the first transmission scanner was only built in the seventies by G. N. Hounsfield [2], who divided the 1979 Nobel Prize with A. M. Cormack who, in 1963, gave fundamental contributions for the development of reconstruction algorithms [3].

2.1 Algebraic Reconstruction Algorithms

A solution for the problem of image reconstruction consists of assuming that the transversal section is an unknown matrix and then to generate algebraic equations in terms of the projection data. The linear model for the image reconstruction can be written by Eq. (1), where g represents the vector of projection data, of size Mx1, f is the vector of the original image of size N^2x1, H is the projection matrix of size MxN^2 and n is the noise vector of size Mx1.

$$g=Hf+n \quad (1)$$

The Algebraic Reconstruction Technique (ART) searches for the solution through the sequential projection, from an initial estimation, onto the set of hyperplanes that are represented by the successive rows of Eq. (1). The Simultaneous Iterative Reconstruction Technique (SIRT) searches for the solution through the mean of the simultaneous projections onto the hyperplanes and tends to give better results in the case of noisy measurements (inconsistent system of linear equations). Although not initially proposed as such, these methods belong to the class of POCS (Projection onto Convex Sets) algorithms, Stark and Yang [4]. The sequential projection method, in terms of closed and convex sets of restrictions (sequential POCS) was proposed for image recovery by Youla and Webb [5] and

implemented for tomographic image reconstruction without noise by Sezan and Stark [6]. The fundamentals of set theoretic estimation are discussed in detail in Combettes [8], where the method of sequential projections is referred as MOSP (Method of Sequential Projections) and the method of parallel projections as MOPP (Method of Parallel Projections).

In the sequential projections method, an initially chosen vector is projected on a restriction set, then the projections onto all the restriction sets is sequentially performed, in a cyclic way. On the other hand, in the parallel projection method, the projections onto all the restriction sets are made in a single iteration and a weighted average of these projections is obtained. If the intersection of the restriction sets is empty, the sequential method does not converge, but oscillates cyclically between the sets. In this case, the parallel projection method converges to a point that minimizes the sum of the squared distances to all sets, according to Combettes and Puh [7].

3. Projection onto Convex Sets (POCS)

Several problems can be described in the form of convex sets restrictions. The solution to these problems should satisfy all the imposed restrictions. Therefore, the search for the desired solution consists of finding a vector that belongs to the intersection of all the restriction sets. If we suppose that there exist n restriction sets, represented by C_i (i=1,2,...,n), the solution to the problem is in the intersection of the sets, represented by Eq. (2):

$$C_0 = \bigcap_{i=0}^{n} C_i \tag{2}$$

3.1 POCS Algorithms

If the sets C_i (i=1,2,...,n) are closed and convex and their intersection C_0 is non-empty, the successive projections on the sets will converge to a vector which belongs to C_0. Eq. (3) represents the sequential POCS algorithm, under the hypothesis that x_0 is any initial vector that represents the initial estimate:

$$x_{k+1} = P_{C_n} \cdots P_{C_2} P_{C_1} x_k \qquad k = 0,1,2,3,\cdots \tag{3}$$

The POCS algorithm can also be implemented in parallel. In this implementation, the vector is projected in all sets simultaneously and to each projection on a set a weight is assigned. Eq. (4) describes the parallel POCS algorithm. Observe that the summation of all weights is equal to one, according to Eq. (5):

$$x_{k+1} = x_k + \sum_{i=1}^{n} w_i \left(P_{C_i} - x_k \right) \qquad k = 0,1,2,3,\cdots \tag{4}$$

$$\sum_{i=1}^{n} w_i = 1 \tag{5}$$

It is possible to control the sequence of sets onto which the projections are made in POCS methods. Censor and Zenios [9] presented six methods to control this sequence: the cyclic control, the quasi-cyclic control, the repetitive control, the most distant sets control, the approximately most distant sets control and the most violated restrictions control.

3.2 Convex Restrictions Sets

By using the projection methods, it is possible to incorporate restrictions into the reconstruction algorithm. Such restrictions are represented by convex and closed sets, which guarantee the convergence of the algorithm. In the following, we present the sets that were used in our work.

Eq. (6) describes the finite support set, where H is a Hibert Space, h is the obtained image and Ω is the region that describes the support.

$$C_{SF} = \{h : h \in H \ \text{and}\ h(x,y) = 0 \ \text{for}\ (x,y) \notin \Omega\} \tag{6}$$

Eq. (7) describes the limited amplitude set.

$$C_{AL} = \{h : h \in H \ \text{and}\ \alpha \le h(i) \le \beta \quad \forall i \in \Omega\} \tag{7}$$

Eq. (8) describes the set of vectors (images) in H that are at a distance less than or equal to ε_R from a reference image f_R.

$$C_R = \{h : h \in H \ \text{and}\ \|h - f_R\| \le \varepsilon_R\} \tag{8}$$

The set given by Eq. (9) describes all vectors which have energy less than or equal to E.

$$C_E = \left\{h : h \in H \quad \text{and} \quad \|h\|^2 \le E = \rho^2\right\} \tag{9}$$

4. Algorithms

We compared four reconstruction methods: a) ART; b) SIRT; c) sequential POCS and d) parallel POCS. For the ART method, the algorithm was described by Eq. (3), while for the SIRT method, the algorithm was given by Eq. (4), where all the sets have the same value for w_i. In these two algorithms the vectors are only projected onto the M hyperplanes that are described by Eq. (1).

For the sequential and parallel POCS methods, the sets of restrictions are given by Eqs. (1), (6), (7), (8) and (9). Eq. (10) describes the sequential POCS algorithm.

Eq. (11) describes the parallel POCS implementation. The first three methods used cyclic control, while the parallel POCS used repetitive control.

$$x_{k+1} = P_{SF} P_{AL} P_E P_R P_M \ldots P_2 P_1 x_k \qquad k = 0,1,2,\cdots \tag{10}$$

$$x_{k+1} = P_{SF} P_{AL} y_{k+1}$$

$$y_{k+1} = z_{k+1} + \frac{1}{2}\left((P_R - z_{k+1}) + (P_E - z_{k+1})\right)$$

$$z_{k+1} = x_k + \frac{1}{M}\sum_{i=1}^{M}\left(P_i x_k - x_k\right) \qquad k = 0,1,2,\cdots \tag{11}$$

5. Experimental Data

Three experimental phantoms were used: homogeneous, asymmetrical and symmetrical. The homogeneous phantom is a cylinder of nylon with water inside it. The asymmetrical phantom is a cylindrical object of nylon, with wholes of different sizes. The symmetrical phantom is a cylindrical object of plexiglass, with two wholes and two cylinders of aluminum inside. The data was obtained with a minitomograph scannner for soil science described by Cruvinel et al [10] with a ^{231} Am radioactive source.

6. Results

The reconstruction of the three phantoms previously described was performed. The images obtained with a low exposure time (three seconds per ray) were considered the noisy reference image. The images reconstructed with the highest exposure (twenty seconds per ray) were considered the ideal image and the images reconstructed from ten seconds up per ray are the noisy images that we want to reconstruct. The reconstructions with limited view were made considering only projections angles between 0^o and 90^o and 0^o and 135^o.

The ideal reconstructed images are shown in Figure 1. In this case the reconstruction was performed with the SIRT algorithm, by also adding the restrictions of non-negativity and finite support.

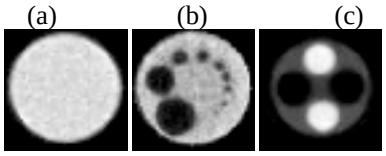

Figure 1: Ideal Phantom Images: (a) homogeneous; (b) asymmetrical; (c) symmetrical

For the reconstruction of the reference images, the same method of the previous paragraph was used. Figure 2 shows the images that were used as reference.

The criterion suggested by Oskouid-Fard and Stark [11] and given by Eq. (12) was used to measure the reconstruction error. In this equation δ_n is the percentual error at the n^{th} iteration, f_n is the n^{th} projection and f is the ideal image.

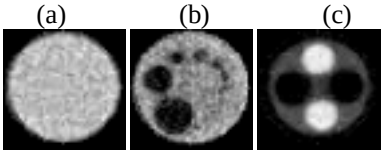

Figure 2: Reference Phantom Images: (a) homogeneous; (b) asymmetrical; (c) symmetrical

$$\delta_n = \frac{\|f_n - f\|}{\|f\|} \times 100 \tag{12}$$

6.1 Reconstruction under noisy data

Figure 3 displays the images of the homogeneous phantom reconstructed with different methods.

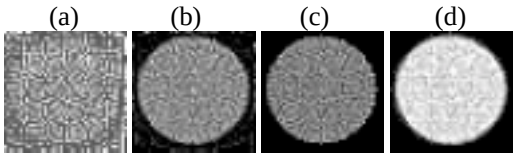

Figure 3: Reconstructed image of the homogeneous phantom with the methods: (a) ART; (b) SIRT; (c) sequential POCS; (d) parallel POCS

Figure 4 and 5 show respectively the asymmetrical and symmetrical phantom reconstructed with the same methods.

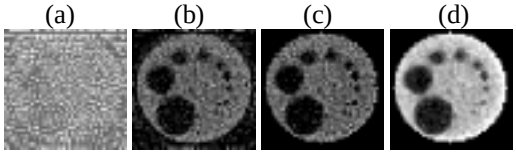

Figure 4: Reconstructed image of the asymmetrical phantom with the methods: (a) ART; (b) SIRT; (c) sequential POCS; (d) parallel POCS

Table 1 shows the percentual error at the 500th iteration.

Phantoms	Homogeneous	Asymmetrical	Symmetrical
ART	301.3	367.4	274.2
SIRT	35.3	59.2	31.3
Sequential POCS	29.0	45.2	19.8
Parallel POCS	10.3	29.0	10.9

Table 1: Percentual error under noisy data at the 500^{th} iteration

(a) (b) (c) (d)

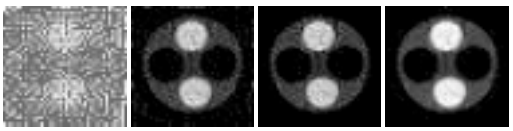

Figure 5: Reconstructed image of the symmetrical phantom with the methods: (a) ART; (b) SIRT; (c) sequential POCS; (d) parallel POCS

6.2 Reconstruction with limited view (0^o and 135^o)

Figure 6 shows the reconstruction of homogeneous phantom obtained with high exposures but with limited view between angles of 0^o and 135^o.

(a) (b) (c) (d)

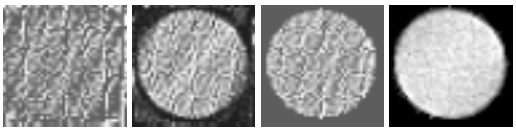

Figure 6: Reconstructed image of the homogeneous phantom with the methods: (a) ART; (b) SIRT; (c) sequential POCS; (d) parallel POCS

Figure 7 shows the reconstruction of asymmetrical phantom with limited view between angles of 0o and 135^o. Figure 8 displays the images of the symmetrical phantom.

(a) (b) (c) (d)

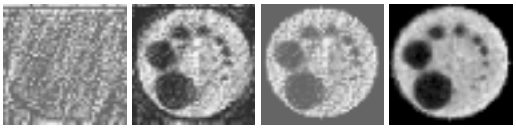

Figure 7: Reconstructed image of the asymmetrical phantom with the methods: (a) ART; (b) SIRT; (c) sequential POCS; (d) parallel POCS

Table 2 shows the percentual error with limited view between angles of 0^o and 135^o at the 500^{th} iteration.

Phantoms	Homogeneous	Asymmetrical	Symmetrical
ART	410.9	468.0	384.2
SIRT	45.7	42.7	41.1
Sequential POCS	43.0	38.2	18.0
Parallel POCS	7.4	7.6	6.3

Table 2: Percentual error under limited view (0^o and 135^o) at the 500^{th} iteration

(a) (b) (c) (d)

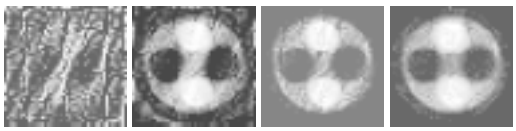

Figure 8: Reconstructed image of the symmetrical phantom with the methods: (a) ART; (b) SIRT; (c) sequential POCS; (d) parallel POCS

6.3 Reconstruction with limited view (0^o and 90^o)

Figure 9 shows the image of the homogeneous phantom reconstructed with limited view (between 0^o and 90^o) using different methods.

(a) (b) (c) (d)

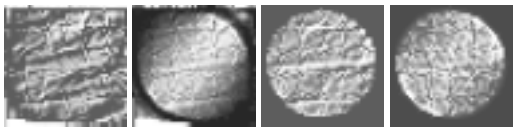

Figure 6: Reconstructed image of the homogeneous phantom with the methods: (a) ART; (b) SIRT; (c) sequential POCS; (d) parallel POCS

Figures 10 and 11 show the reconstruction of asymmetrical and symmetrical phantoms with limited view (between 0o and 90^o).

(a) (b) (c) (d)

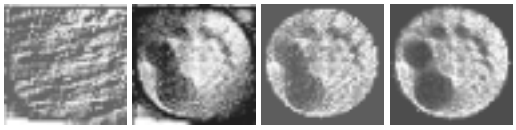

Figure 7: Reconstructed image of the asymmetrical phantom with the methods: (a) ART; (b) SIRT; (c) sequential POCS; (d) parallel POCS

Table 3 shows the percentual error with limited view for angles between 0^o and 90^o. at the 500^{th} iteration.

Phantoms	Homogeneous	Asymmetrical	Symmetrical
ART	462.5	437.2	339.9
SIRT	68.5	66.1	57.1
Sequential POCS	26.7	45.6	35.7
Parallel POCS	9.2	17.5	7.4

Table 3: Percentual error under limited view (between0^o and 90^o) at the 500^{th} iteration

(a) (b) (c) (d)

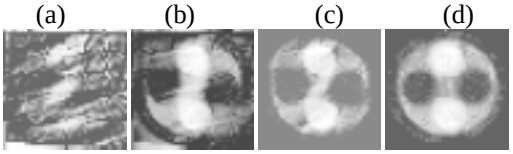

Figure 8: Reconstructed image of the symmetrical phantom with the methods: (a) ART; (b) SIRT; (c) sequential POCS; (d) parallel POCS

7. Conclusions

By analysing the data that was obtained with the comparative study, it is possible to note that, the parallel POCS method obtained the best visual and numerical results not only in the presence of noise but also under limited view. The sequential POCS displays somewhat better numerical results than the SIRT , but substantially better visual results. Note in Figure 4, for example, the superior resolution of the sequential POCS on the small holes, or the visual results for angles between 0^o and 90^o. The worst visual and numerical results were obtained with the ART. This is a consequence of the use of adequate a priori information by the sequential and parallel POCS methods to overcome the ill-conditioning of the noisy and limited view reconstruction problems.

In the presence of noise, there is no intersection of the restriction sets. It was observed that the sequential methods do not converge, but oscillate among the different restriction sets, on the same iteration. This does not happen with the parallel methods.

It should be observed that the imposed restrictions on the POCS (sequential and parallel) assure convergence of the results. With the ART and the SIRT methods (that rely only on the projected data, with no a priori information), however, there is a tendency for divergence of δ_n as the number of iterations increases.

Acknowledgement

The work of Fernando V. Salina was supported by a CAPES scholarship.

References

[1] J. Radon. "On the Determination of Functions from their Integrals along Certain Manifolds", *Ber. Saechs. Akad. Wiss, Leipzig Math. Phys*. 69 (1917), 262-277.

[2] G.N Hounsfield. "Computerized Transverse Axial Scanning (Tomography) I: Description of System", *Brit. J. Radiol* 46 (1973), 1016-1022.

[3] A. M. Cormack. "Representation of a Function by Its Line Integrals, with some Radiological Applications", *J. Appl. Physics* 34 (1963),2722-2727.

[4] H. Stark and Y. Yang. *Vector Space Projections – A Numerical Approach to Signal and Image Processing, Neural Nets, and Optics*, John Wiley & Sons, 1998.

[5] D. C. Youla and H. Webb. "Image Restoration by the Method of Convex Projections: Part1 – Theory", *IEEE Trans. Med. Imaging, MI-1* (1982), 81-94.

[6] M. I. Sezan. and H. Stark. "Image restoration by the method of convex projections: part2- Applications and numerical results", *IEEE Trans. Medical Imaging l. MI-1* (1982), 95-101.

[7] P. L. Combettes and H. Puh. "Parallel Projection Methods for Set Theoretic Signal Reconstruction and Restoration", *ICASSP, Vol 5* (1993), 297-300.

[8] P. L. Combettes. "The Convex Feasibilty Problem in Image Recovery", *Advances in Imaging and Electron Physics* .95 (1996),155-270.

[9] Y. Censor and S. A. Zenios. *Parallel Optimization – Theory, Algorithms, and Application*, Oxford University Press, 1997

[10] P. E. Cruvinel.; R. Cesareo, R. Crestana, and S. Mascaenhas, "X and γ Rays Computerized Minitomograph Scanner for Soil Science", *IEEE Trans. on Instrum. and Measur. 39* (1990), 745-750.

[11] P. E. Oskoui-Fard and H. Stark. "Tomographic Image Reconstruction Using the Theory of Convex Projections", *IEEE Transactions on Medical Imaging l v7* (1998), 45-58.